

Research Paper

Novel spheroid reservoir bioartificial liver improves survival of nonhuman primates in a toxin-induced model of acute liver failure

Yi Li^{1,2,3,4*}, Qiong Wu^{1*}, Yujia Wang^{1,2,3}, Chengxin Weng⁵, Yuting He¹, Mengyu Gao¹, Guang Yang⁶, Li Li¹, Fei Chen¹, Yujun Shi¹, Bruce P. Amiot², Scott L. Nyberg^{2, 3}, Ji Bao¹, Hong Bu¹

1. Laboratory of Pathology, Key Laboratory of Transplant Engineering and Immunology, NHFPC, West China Hospital, Sichuan University, Chengdu 610041, Sichuan, China
2. Department of Surgery, Mayo Clinic, Rochester, MN, USA
3. William J. von Liebig Center for Transplantation and Clinical Regeneration, Mayo Clinic, Rochester, MN, USA
4. Precision Medicine Key Laboratory, West China Hospital, Sichuan University, Chengdu 610041, Sichuan, China
5. West China School of Medicine, Sichuan University, Chengdu 610041, Sichuan, China
6. Experimental Animal Center, West China Hospital, Sichuan University, Chengdu 610041, China

* The authors provided equal contribution to this work.

 Corresponding authors: Ji Bao, PhD. E-mail: baoji@scu.edu.cn. Hong Bu, MD. PhD. E-mail: hongbu@scu.edu.cn. Laboratory of Pathology, West China Hospital, Sichuan University, 37# Guoxue Road, Chengdu 610041, Sichuan Province, China. Tel.: +86-28-85164030. Fax: +86-28-85164034.

© Ivyspring International Publisher. This is an open access article distributed under the terms of the Creative Commons Attribution (CC BY-NC) license (<https://creativecommons.org/licenses/by-nc/4.0/>). See <http://ivyspring.com/terms> for full terms and conditions.

Received: 2018.04.07; Accepted: 2018.10.10; Published: 2018.11.09

Abstract

This study aims to evaluate the effectiveness and safety of the spheroid reservoir bioartificial liver (SRBAL) with porcine hepatocyte organoids in a preclinical nonhuman primate model of acute liver failure (ALF).

Methods: Thirty healthy rhesus monkeys were infused with α -amanitin and lipopolysaccharide and randomized into five groups (ALF alone control group; sham no-cell SRBAL treatment group; groups A, B and C with SRBAL treatment started at 12 h, 24 h and 36 h after induction of ALF, respectively). Animals were continuously treated with the SRBAL device for 6 h and followed for up to 336 h.

Results: Survival of ALF monkeys improved with hepatocyte SRBAL treatment compared to control groups. Blood ammonia and total bilirubin were lower, and albumin levels were higher in all hepatocyte SRBAL treatment groups. No evidence of porcine endogenous retrovirus was identified in monkey liver or blood after SRBAL treatment. Titers of monkey antibody (IgG, IgM) did not rise after SRBAL treatment. In survival cases, the proportion of necrotic and apoptotic hepatocytes was lower in SRBAL-treated groups, with earlier liver regeneration leading to recovery. Cytokines TNF- α , IL-6, IL-12, IL-1 β , IL-8, IFN- γ and IL-2 were ameliorated by the SRBAL treatment, while levels of M-CSF; HGF, EGF and VEGF; IL-1RA and MIF rose on priming, proliferation and the late phase of liver regeneration.

Conclusions: The benefit of SRBAL therapy included preventive effects and therapeutic effects. SRBAL improved survival rate and prolonged median survival time in a nonhuman primate model of drug-induced ALF, and these benefits declined with a delay in the initiation of therapy. Improved survival and recovery of ALF monkeys was associated with a reduction in blood ammonia levels, inhibition of the pro-inflammatory response of ALF, and provided a microenvironment more suitable for regeneration of the injured liver.

Key words: acute liver failure, bioartificial liver, hepatocyte, organoid, *Macaca mulatta*

Introduction

Acute liver failure (ALF) is defined by the acute presentation of coagulopathy, jaundice and hepatic encephalopathy (HE) in the absence of pre-existing liver disease. ALF is associated with a high mortality rate exceeding 50% [1]. Orthotopic liver transplantation is the only proven therapy for ALF, but its overall usage is limited by the need for major surgery, life-long immunosuppression, and the shortage of donor organs. The expanding gap between the number of patients on the waiting list for liver transplantation and available donor livers has highlighted the strong need for alternative therapies, especially in the setting of ALF [2].

New therapies, including cell transplantation, such as hepatocyte transplantation and stem cell transplantation, tissue engineered livers and liver support systems are currently under investigation. Among them, liver support systems including acellular artificial liver (AL) devices and cell-based bioartificial liver (BAL) devices have been developed with a promising goal of supplementing liver function [3]. Both options are intended to bridge patients with liver failure to transplantation or to allow the native liver time for spontaneously recover through regeneration.

Molecular adsorbents recirculating system (MARS) is a widely used AL device. It was designed as a multi-circulation purification system with continuous detoxification of albumin-bound toxins. Many studies have demonstrated the ability of MARS to remove toxins, and thus ameliorate symptoms of HE. Other studies have suggested an improved survival rate during ALF; however, improved survival of MARS has not yet been demonstrated in a prospective randomized clinical trial [4, 5]. Despite evidence of beneficial improvements, the lack of metabolic and synthetic activity by MARS limits its effectiveness and may expose the ALF patients to a risk of thrombocytopenia and coagulopathy.

In contrast, bioartificial liver (BAL) devices are composed of living cells that can perform the numerous functions of a normal liver [6]. Our improved spheroid reservoir bioartificial liver (SRBAL) contains porcine hepatocyte-HUVEC spheroids, termed organoids, that conduct comprehensive metabolism, synthesis and effective detoxification [7]. SRBAL makes use of a hollow fiber cartridge membrane to allow passage of toxins, proteins and other waste substances without exchange of larger blood components from the patient or hepatocytes from the SRBAL. In a previous preclinical study involving ALF pigs, SRBAL exhibited effective ammonia clearance associated with

neuroprotection and a reduction in both intracranial pressure (ICP) and brain edema [8, 9]. The possibility of xeno-zoonosis, such as porcine endogenous retrovirus (PERV) transmission, was not addressed in the prior study. Further investigation of SRBAL therapy in a primate species could better address the possibility of PERV transmission during exposure to porcine hepatocytes and provide supporting data to determine the therapeutic benefit of SRBAL therapy prior to its clinical application.

We have established a nonhuman primate model of ALF using intraperitoneal administration of α -amanitin and lipopolysaccharide (LPS) in *Macaca mulatta* (rhesus) monkeys [10]. In the current randomized prospective preclinical study, primary porcine hepatocytes were co-cultured with human umbilical vein endothelial cells (HUVECs) as the cell source for SRBAL. Our experimentation was designed to answer the following questions: 1. Does SRBAL treatment improve survival of ALF rhesus monkeys? 2. Are the levels of ammonia, bilirubin, liver enzymes and cytokines influenced by SRBAL and associated with improved outcome of ALF? 3. What is the therapeutic mechanism of SRBAL for ALF? Answers to these questions are needed to establish a mechanistic role for cell-based liver support therapy and to design future clinical trials of SRBAL.

Methods

All experimental protocols were approved by the Institutional Animal Care and Use Committee (IACUC), Animal Experiment Center of Sichuan University (Approval No. 2016063A) and met institutional and national guidelines. All animals were cared for in accordance with the requirements of the Laboratory Animal Welfare Act and amendments thereof.

Animals

Male Bama miniature pigs aged 3 months (8-10 kg) were purchased from the Animal Experiment Center of Sichuan University (Chengdu, China). High protein diet (40%) and water were given for 7 days before hepatocytes isolation.

Male rhesus monkeys aged 5-7 years (10-20 kg) were purchased from Safe and Secure Experimental Animal Breeding Base (Chengdu, China). Standard laboratory chow and water were given ad libitum. All animals were housed in singular standard cages in an air-conditioned room (21-25 °C), with a 12 h light/dark cycle.

Hepatocyte-HUVEC organoids formation

Hepatocytes were isolated from male Bama miniature pigs using a modified three-step

collagenase perfusion method as described elsewhere [11]. The digested liver tissue was then gently split to allow cell dispersion and the collected cell suspension was filtered through four layers of gauze. Hepatocytes were washed three times with ice-cold wash media and centrifuged at 4 °C for 10 min at 50 ×g.

HUVECs were kindly provided by State Key Laboratory of Biotherapy, Sichuan University. Cells were cultured in high glucose Dulbecco's Modified Eagle's Medium (DMEM, Invitrogen, Carlsbad, CA) containing 10% FBS.

In co-culture conditions, porcine hepatocytes (5×10^6 /mL) and HUVECs (5×10^4 /mL) were mixed in 1000 mL of serum-free medium (SFM) [12] immediately before inoculation into four spheroid generation chambers. Spheroid chambers were incubated at 37 °C in a humidified atmosphere, supplied with 5% carbon dioxide gas mixture, and rocked continuously at 0.12 Hz for 24 h [12].

SRBAL treatment of ALF monkeys

Thirty rhesus monkeys were divided into five groups: 1) Group A (n=6), SRBAL treatment was initiated 12 h after administration of toxin; 2) Group B (n=6), SRBAL treatment was initiated 24 h after administration of toxin; 3) Group C (n=6), SRBAL treatment was initiated 36 h after administration of toxin; 4) Group D (n=6), sham no-cell SRBAL treatment without hepatocytes was initiated 12 h after administration of toxin; 5) Group E (n=6), ALF-alone group, animals received standard intensive care alone after administration of toxin.

ALF was induced in the rhesus monkeys with intraperitoneal administration of 0.1 mg/kg α -amanitin (Sigma-Aldrich, CA, USA) and 1.0 μ g/kg lipopolysaccharide (LPS, Sigma-Aldrich) as described elsewhere [10]. Animals were then allowed to move and eat freely in cages.

During treatment, animals in all groups were anesthetized with intramuscular administration of Zoletil 50 (10 mg/kg body weight, Virbac, France) and sedation was maintained with propofol (6 mg/kg/h, Qingyuanjiabo, Guangdong, China). Rhesus monkeys in groups A-D underwent placement of a central venous catheter (16 G, Puyi, Shanghai, China) in the femoral vein as blood outflow and a catheter (20 G) in the peripheral vein as blood inflow. The bioreactor of SRBAL device was inoculated with hepatocyte-HUVEC organoids. The animals were connected to the SRBAL as shown in **Figure 1A** and treated for 6 h. Animals were recovered and then received standard care for one week to allow healing of incisions and to confirm health status.

PERV RNA and DNA detection

Total RNA was prepared from porcine hepatocytes and peripheral blood mononuclear cells (PBMCs) from the monkeys in all groups with Trizol (Invitrogen) and was reverse transcribed to cDNA using iScript cDNA Synthesis Kit (Bio-Rad, Hercules, CA). RT-PCR was carried out using SsoFast Eva Green Supermix Kit (Bio-Rad) according to the instructions.

Total DNA was extracted from porcine hepatocytes and PBMCs from the monkeys with E.Z.N.A.® DNA Extraction Kit (Omega, CA, USA) and amplified using Taq PCR Master Mix Kit (Qiagen, CA, USA) in accordance with the manual. The products were loaded on 2% agarose gel and visualized by GoldView nucleic acid staining solution.

DNA was further prepared using the droplet digital PCR (ddPCR) Supermix (Bio-Rad) for generation and amplification of sample droplets according to the manufacturer's protocol, then read by a digital droplet (dd)PCR system (QX200, Bio-Rad, CA, USA). The signals from different samples were counted and redistributed according to Poisson's algorithm.

Parameters

After ALF induction, all monkeys were monitored every 12 h for the first 48 h and every 24 h for the remainder of the study. During the 6 h treatment, animals were monitored every hour (**Figure 1B**). Vital signs were recorded by cardiogram monitoring. Blood samples were collected for subsequent analyses. Serum biochemistry was assayed using a chemistry analyzer AU5800 series (Beckman Coulter). Ammonia concentrations were quantified by a blood ammonia assay kit (Nanjing Jiancheng, Nanjing, China). S-100 β proteins have emerged as a biomarker of blood-brain barrier (BBB) permeability and neuropathological conditions including encephaledema and increased ICP [13, 14]. Thus, elevated S-100 β levels were measured using an ELISA kit (Ruikesi, Chengdu, China). Rhesus IgG and IgM levels were detected using ELISA kits (Ruikesi). All the kits were analyzed with a MQX 200 microplate reader (BioTek Instruments Inc., VT, US). Cytokines were assessed using a Luminex 100 instrument with xPONENT 3.1 software using Monkey Cytokine Magnetic 29-Plex Panel (Invitrogen, CA, US).

Histology

Liver tissues were collected for histochemistry and immunohistochemistry to determine the effects of SRBAL treatment on liver necrosis, apoptosis, phagocytosis and regeneration. Liver tissue was

obtained by needle biopsies from ALF monkeys at multiple time points: before drug infusion, 48 h after drug infusion, 48 h after sham treatment and at 48 h, 168 h and 336 h after SRBAL treatments. Liver tissue was fixed in 10% formalin and then embedded in paraffin. All specimens were analyzed by hematoxylin and eosin (HE) staining, active caspase-3 staining (cleaved caspase-3 antibody, Affinity Biologicals, Ancaster, Canada), CD68 staining (anti-CD68 antibody, Abcam, Cambridge, UK) and Ki-67 staining (anti-Ki-67 antibody, Abcam, Cambridge, UK).

Statistics

Data are presented as mean \pm SEM. Statistical analysis was performed using one-way ANOVA and Dunnett's t test. Survival time was analyzed using Kaplan-Meier, and significance was tested with the log-rank test. A level of $p < 0.05$ was accepted as significant. All data were analyzed with SPSS software version 17.0.

Results

Hepatocyte organoids formation

Porcine hepatocytes from one donor mini pig were harvested (Figure 2A) and co-cultured with the HUVECs in the rocker system to form hepatic organoids (Figure 2B). The average initial total cell yield of fresh suspension from all pigs reached $(2.56 \pm 0.41) \times 10^{10}$ cells. Cell viability of hepatic organoids was greater than 98% (Figure 2C). Over 94% of organoids were $>50 \mu\text{m}$ diameter after 24 h culture (Figure 2D). All the organoids were used for one SRBAL treatment. Organoids preserved higher levels of liver-specific genes including *alb*, *lmf4*, *g6pc* and *cyp3a7* (Figure 2E). Average rates of oxygen consumption ($184.3 \pm 1.9 \mu\text{mol}/\text{min}$), albumin production ($1944.6 \pm 84.5 \text{ ng}/\text{h}$), and urea synthesis ($63.3 \pm 0.6 \text{ mg}/\text{h}$) were determined after 30 min of equilibration in the SRBAL reservoir, indicating high viability and active functionality of hepatocyte organoids prior to treatment (Figure 2F-H).

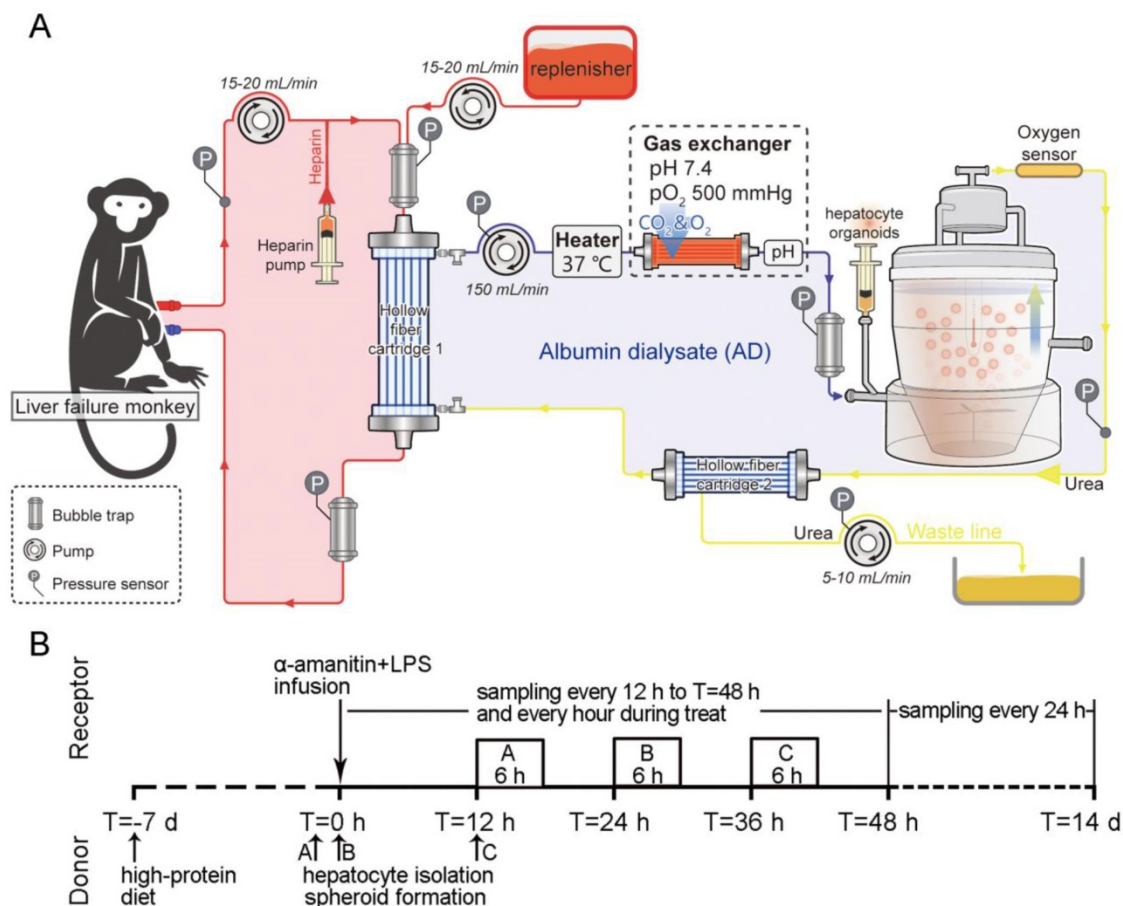


Figure 1. Experimental design. (A) Schematic of the extracorporeal circuit including the SRBAL apparatus. The red line indicates the blood compartment, while the yellow/blue lines indicate the acellular albumin dialysate (AD) compartment. Pressures, temperature and oxygen pressure were detected by respective sensors. Flow rates were determined by pumps. The semipermeable membrane of hollow fiber cartridge 1 was used to diffuse and convect waste molecules from blood to the treatment medium. An oxygenator was used to maintain the inlet oxygen tension above 500 mmHg. The spheroid reservoir functioned as a suspension bioreactor containing hepatocyte organoids with fluid entering its bottom and exiting its top. Hollow fiber cartridge 2 was used to maximize removal of detoxification products and redundant fluid in the AD circuit. (B) Experimental timeline showing the sequence of events of pig donors and monkey receptors and initial time of treatments of groups A, B and C.

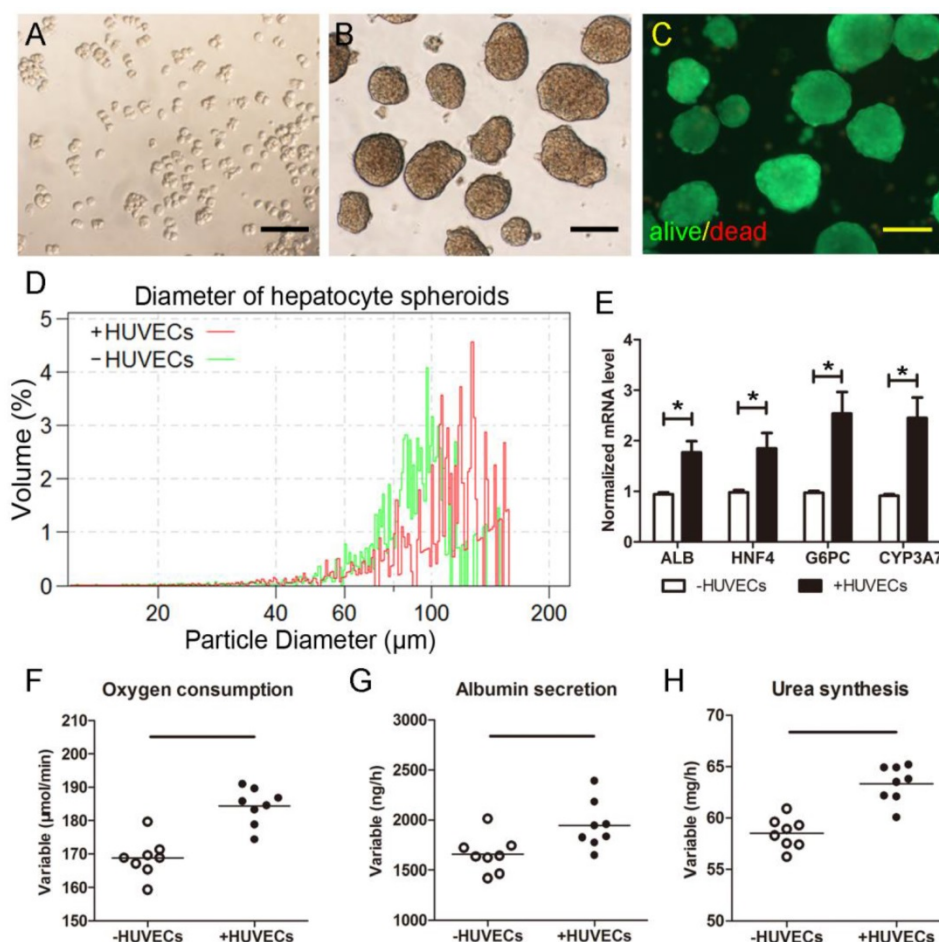


Figure 2. Morphology of isolated porcine hepatocytes. (A) Freshly isolated hepatocytes. **(B)** Hepatocyte spheroids formed after 24h rocker culture. **(C)** Viability Fluoroquench staining of hepatocyte spheroids after 24h rocker culture (green: live cells; red: dead cells). **(D)** Diameter measurement of hepatocyte organoids using Multisizer after 24h rocker culture. **(E)** Expressions of liver-specific genes including *alb*, *hnf4*, *g6pc* and *cyp3a7*. **(F)** Oxygen consumption, **(G)** albumin production and **(H)** urea synthesis of newly-formed hepatocyte organoids in SRBAL reservoir for the first half hour of adaptive culture ($2.41 \pm 0.38 \times 10^{10}$ cells). * $p < 0.05$. Scale bar = 100 μm.

Survival

None of the animals in the ALF control group survived beyond 68 h. The median survival time (MST) of the ALF control group was 60.5 h, whereas the MST of the sham SRBAL group was 90 h. In contrast, animals in the SRBAL treatment groups survived longer. The MST was significantly prolonged in the 12 h SRBAL group (336 h, $p < 0.0001$). The MSTs of the 24 h SRBAL and 36 h SRBAL groups were 248 h and 131.5 h ($p < 0.0001$) respectively, both shorter than that of the 12 h SRBAL group ($p < 0.0001$) (Figure 3A). This result also proved that earlier treatment had a better outcome.

Immunoreactivity evaluation

The levels of IgM in rhesus blood were increased 3-4-fold 24 h after administration of α -amanitin and LPS but declined to normal level by the end of the experiment (336 h) (Figure 3B). The levels of IgG in rhesus blood did not increase significantly (Figure 3C).

Agarose gel electrophoresis revealed no PERV DNA in PBMCs of monkeys exposed to pig hepatocytes by SRBAL treatment (Figure 3D). The ddPCR assay did not detect copy numbers of PERV in PBMCs and liver tissue of monkeys (Figure 3E). Quantitative assessment in RT-PCR showed no PERV mRNA in monkey PBMCs in all groups at 12 h after initiation of treatment (Figure 3F).

Treatment efficacy

Animal survival was influenced by the timing of SRBAL therapy after induction of ALF. All six rhesus monkeys in the 12 h SRBAL group were eating and drinking within 3 days after SRBAL treatment; these group A animals moved freely within 7 days and all survived to 14 days. Fifty percent (3 of 6) of group B monkeys and 17% (1 of 6) of group C monkeys survived to 14 days. All ten animals who survived to 14 days remained healthy at 1 year. In contrast, none of the control animals in sham group or ALF group survived to 14 days.

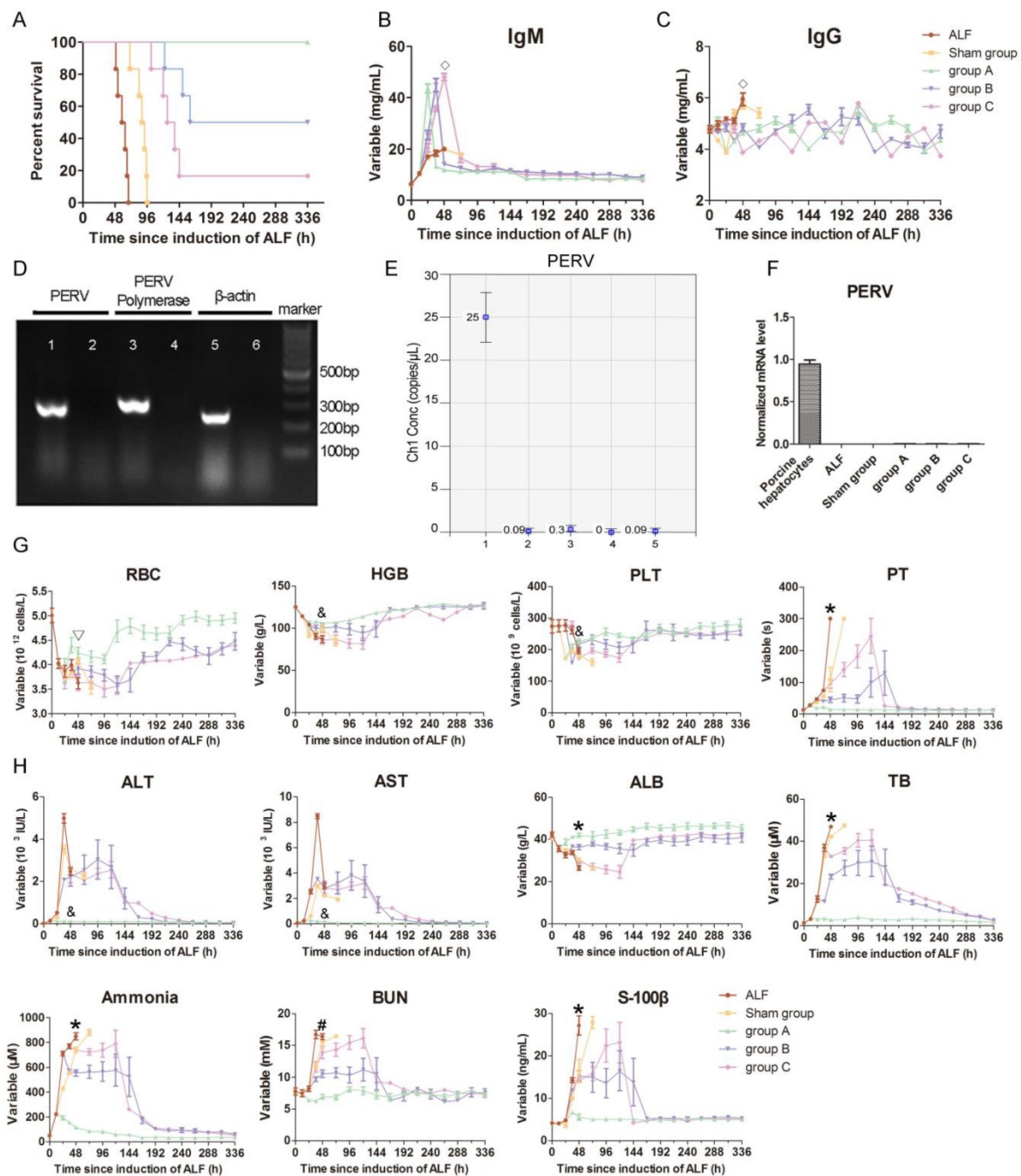


Figure 3. Evaluation of SRBAL therapy. (A) Survival curves of all five conditions. Survival rate and median survival time (MST) of monkeys treated with SRBAL were improved in group A (100%, MST = 336 h, $p < 0.001$), group B (50%, MST = 248 h, $p < 0.001$) and group C (17%, MST = 131.5 h, $p < 0.001$) compared to those of the two control groups, sham (0%, MST = 90 h) and ALF (0%, MST = 60.5 h). (B) IgM and (C) IgG antibody levels in monkey blood before and after SRBAL treatments. (D) Electrophoresis results of the PERV DNA extracted from porcine hepatocytes and monkey PBMCs. Sample 1, 3, 5; porcine liver; Sample 2, 4, 6; rhesus monkey blood. (E) Droplet digitalPCR (ddPCR) results of the PERV DNA extracted from porcine hepatocytes and monkey PBMCs and liver. Sample 1: pig liver; Sample 2, 3: monkey liver; Sample 4, 5: monkey blood. (F) RT-PCR results of the PERV mRNA extracted from porcine hepatocytes and monkey PBMCs. (G) Hematological parameters including red blood cell (RBC), hemoglobin (HGB), platelet (PLT) and prothrombin time (PT). (H) Biochemical parameters including alanine aminotransferase (ALT), aspartate aminotransferase (AST), albumin (ALB), total bilirubin (TB), ammonia, blood urea nitrogen (BUN) and S-100 β . $\diamond p < 0.05$ groups A, B, C versus ALF control group; * $p < 0.05$ sham group, groups A, B, C versus ALF control group; $\nabla p < 0.05$ sham group, group A versus ALF control group; & $p < 0.05$ group A versus ALF control group; # $p < 0.05$ groups A, B versus ALF

As summarized in Figure 3G-H, all animals showed marked increases in PT, ALT, AST, TB and ammonia, and a significant decrease in ALB level 12 h after α -amanitin and LPS administration. The ammonia levels of animals in the ALF and sham

treatment groups increased significantly and reached $850.0 \pm 28.1 \mu\text{M}$ and $740.0 \pm 21.2 \mu\text{M}$ at 48 h after drug administration, respectively. In the treatment group, the ammonia levels decreased to $114.8 \pm 9.6 \mu\text{M}$ in group A, $556.2 \pm 25.5 \mu\text{M}$ in group B and $738.8 \pm 13.0 \mu\text{M}$

in group C at 48 h after drug administration.

The TB levels in the ALF and sham groups increased significantly and reached $46.9 \pm 1.8 \mu\text{M}$ and $42.2 \pm 1.3 \mu\text{M}$ at 48 h after drug administration. Meanwhile, the TB levels decreased to $2.8 \pm 0.6 \mu\text{M}$ in group A, $23.4 \pm 2.4 \mu\text{M}$ in group B and $32.9 \pm 1.1 \mu\text{M}$ in group C at 48 h after drug administration.

The albumin levels were $26.5 \pm 2.3 \text{ g/L}$ and $30.7 \pm 1.6 \text{ g/L}$ in the ALF and sham groups, respectively. In contrast, the levels of albumin were $41.9 \pm 2.2 \text{ g/L}$ in group A, $36.3 \pm 2.6 \text{ g/L}$ in group B, and $29.6 \pm 2.0 \text{ g/L}$ in group C at 48 h after drug administration.

The S-100 β levels in the ALF and sham groups increased significantly and reached $27.1 \pm 5.0 \text{ ng/mL}$ and $16.4 \pm 6.0 \text{ ng/mL}$ at 48 h after drug administration. However, the S-100 β levels decreased to $5.5 \pm 1.6 \text{ ng/mL}$ in group A, $15.4 \pm 2.8 \text{ ng/mL}$ in group B and $14.3 \pm 1.2 \text{ ng/mL}$ in group C at 48 h after drug administration.

Other laboratory parameters were improved during (Table S1) and after the treatment (Figure 3G-H and Figure S1) with significance.

ALF liver histology

All liver tissue from study monkeys appeared normal before drug infusion. Extensive parenchymal hemorrhagic necrosis and steatosis was observed at 48 h after toxin infusion in ALF control group animals. The livers were still extensively necrotic with obvious bleeding across the entire lobule after sham treatment with a no-cell device. The necrosis was notably alleviated by SRBAL treatment with hepatocyte organoids in group A at 48 h. Vacuoles appeared in the pale cytoplasm, and cytoplasmic borders were indistinct in groups B and C. These lesions were gradually reversed at 168 h and 336 h after drug administration in surviving animals (Figure 4A-A'').

Active caspase-3 staining for hepatocyte apoptosis was scarcely observed in healthy liver. Apoptosis was intense in ALF and sham groups at 48 h after drug infusion, according to numerous positive cells. In experimental groups, the caspase-3 expression levels were lower after the SRBAL treatment at the same time point. Positive staining for caspase-3 can still be occasionally observed in some inflammatory cells after the repair at 168 h and 336 h (Figure 4B-B'').

CD68 is a useful marker for the macrophage lineage. CD68 staining showed the Kupffer cells (KCs) lined the walls of the sinusoids in the liver. CD68-positive cells were intensively recruited and activated after the ALF induction. The SRBAL treatment alleviated the overwhelming recruitment of CD68-positive cells. In experimental groups, the

levels of CD68-positive cells were lower after the treatments at 48 h after drug infusion. After the vigorous process of phagocytosis, the dead cells were cleared, and numbers of KCs dropped back to normal (Figure 4C-C'').

Staining of the regenerative marker Ki-67 was rare in normal livers and a small number of proliferating hepatocytes were observed in ALF and sham groups. The SRBAL treatments with hepatocyte organoids increased significantly the percentage of proliferating cells in group A at 48 h after drug administration. The proliferation completed before 168 h. Most of the proliferated cells were located in the area that had normal hepatocyte morphology in groups B and C at 48 h. There were still hepatocytes proliferating at 168 h and 336 h in groups B and C after drug administration (Figure 4D-D'').

Cascade of inflammatory cytokines

Strong inflammatory responses were observed, as evidenced by significant increases in the levels of TNF- α and secondary pro-inflammatory cytokines including IL-6, IL-12, IL-1 β , IL-8, IFN- γ and IL-2. This suggested intense activation of KCs during the development of ALF. Serum levels of these inflammatory cytokines decreased after SRBAL treatment. However, IL-10, an anti-inflammatory cytokine, did not show a significant increase during SRBAL treatment, demonstrating that the survival benefit did not depend on establishing a counter-regulatory homeostasis to prevent overwhelming inflammation (Figure 5A and Figure 6).

Macrophage colony-stimulating factor (M-CSF) is a cytokine that is the primary regulator of macrophage survival, proliferation and differentiation. Although significant increases of M-CSF were observed in all groups after ALF induction, higher levels of M-CSF were detected in SRBAL treatment groups, especially in group A. This demonstrated that the lower levels of M-CSF were associated with the higher deaths, compared with those in the survival cases (Figure 5B and Figure 6).

There were later peaks in growth factors including HGF, EGF and VEGF. According to histological evaluation, proliferation and recovery had started at 48 h. HGF and EGF promoted hepatocyte proliferation, while VEGF stimulated angiogenesis, through binding their receptors on the surface of hepatocyte and endothelial cells respectively (Figure 5B and Figure 6).

IL-1 receptor antagonist (IL-1RA) can inhibit the activities of IL-1 β [15], while macrophage migration inhibitory factor (MIF) plays an important role in the regulation of macrophage function [16]. Up-regulated

expressions of IL-1RA and MIF were observed in groups A, B and C (Figure 5C and Figure 6). This

result suggested these cytokines have a role in mitigating the inflammatory response.

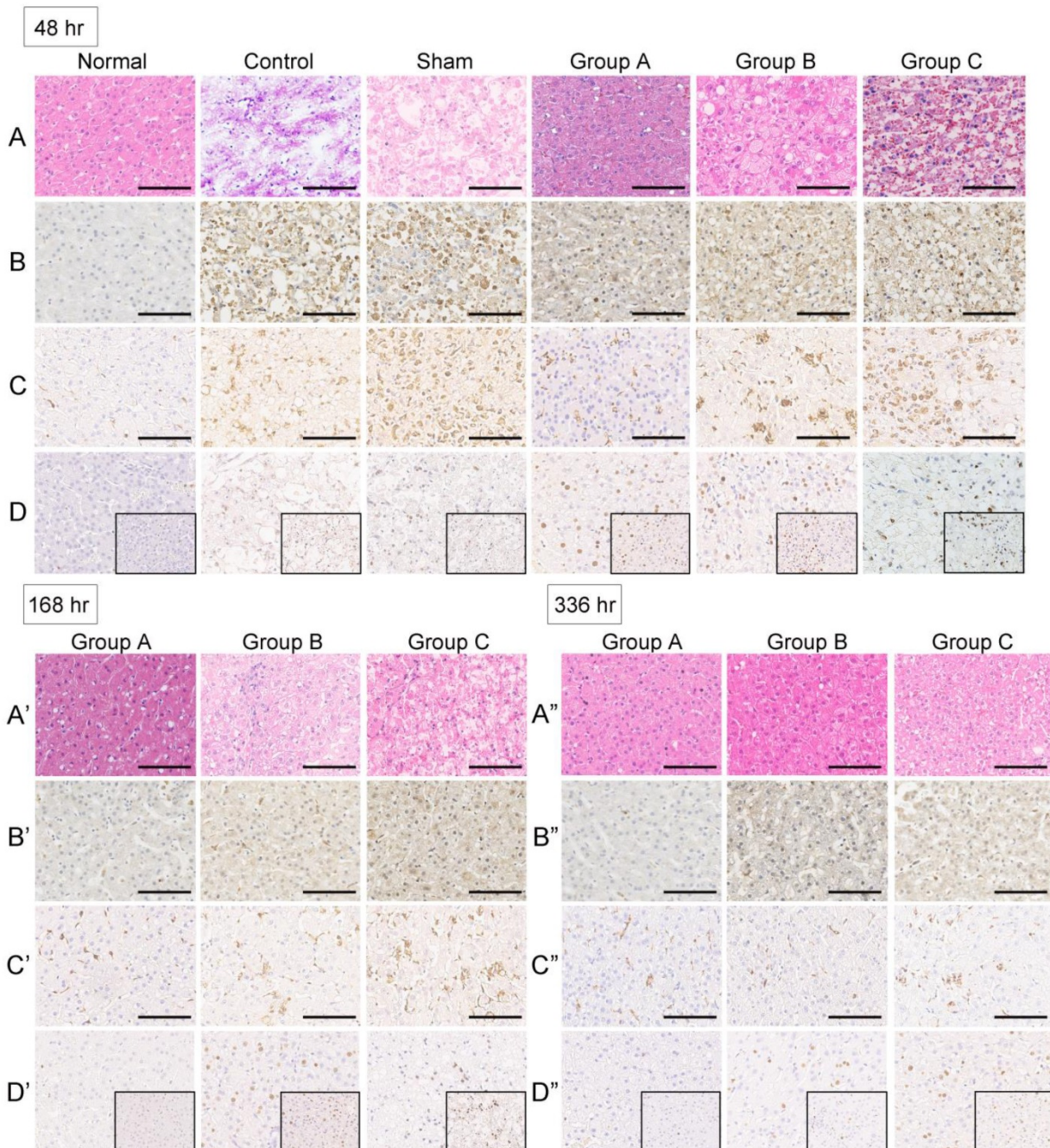


Figure 4. Histology and immunohistochemistry of monkey liver biopsies. (A-A'') No changes in organizational structure and cell morphology were observed in all groups before ALF. Extensive parenchymal hemorrhagic necrosis and steatosis was observed at 48 h after toxin infusion in the control group. The livers were still extensively necrotic with obvious bleeding across the entire lobule after sham treatment with a no-cell device at 48 h after toxin infusion. The numbers of hepatocytes and hepatic parenchymal cells increased significantly after SRBAL treatment at 48, 168 and 336 h after toxin infusion (H&E, $\times 20$). (B-B'') Active caspase-3 staining for hepatocyte apoptosis was scarcely observed in healthy liver. The percentage of caspase-3-positive cells was increased in the ALF and sham groups at 48 h after drug infusion. In the experimental groups, the caspase-3 expression levels were lower after SRBAL treatment at the same timepoint. Caspase-3-positive staining can still be occasionally observed in some inflammatory cells after the repair at 168 h and 336 h (cleaved caspase-3, $\times 20$). (C-C'') CD68 staining showed KCs lining the walls of the sinusoids in the liver. CD68-positive cells were intensively recruited and activated after ALF induction. SRBAL treatment alleviated the overwhelming recruitment of CD68-positive cells. In the experimental groups, the levels of CD68-positive cells were lower after the treatments at 48 h after drug infusion. After the vigorous process of phagocytosis, the dead cells were cleared, and the numbers of KCs dropped back to normal (CD68, $\times 20$). (D-D'') Staining of the regenerative marker Ki-67 was rare in normal livers and a small number of proliferating hepatocytes was observed in the remaining cells in the ALF and sham groups. Remarkable liver regeneration was observed after SRBAL treatment at 48, 168 and 336 h after toxin infusion. The SRBAL treatments with hepatocyte organoids increased significantly the percentage of proliferating cells in group A at 48 h after drug administration. The proliferation completed before 168 h. Most of the proliferated cells were located in the hepatocytes that had normal morphology in groups B and C at 48 h. There were still hepatocytes proliferating at 168 h and 336 h in groups B and group C after drug administration (Ki-67 staining, $\times 20$ and $\times 40$).

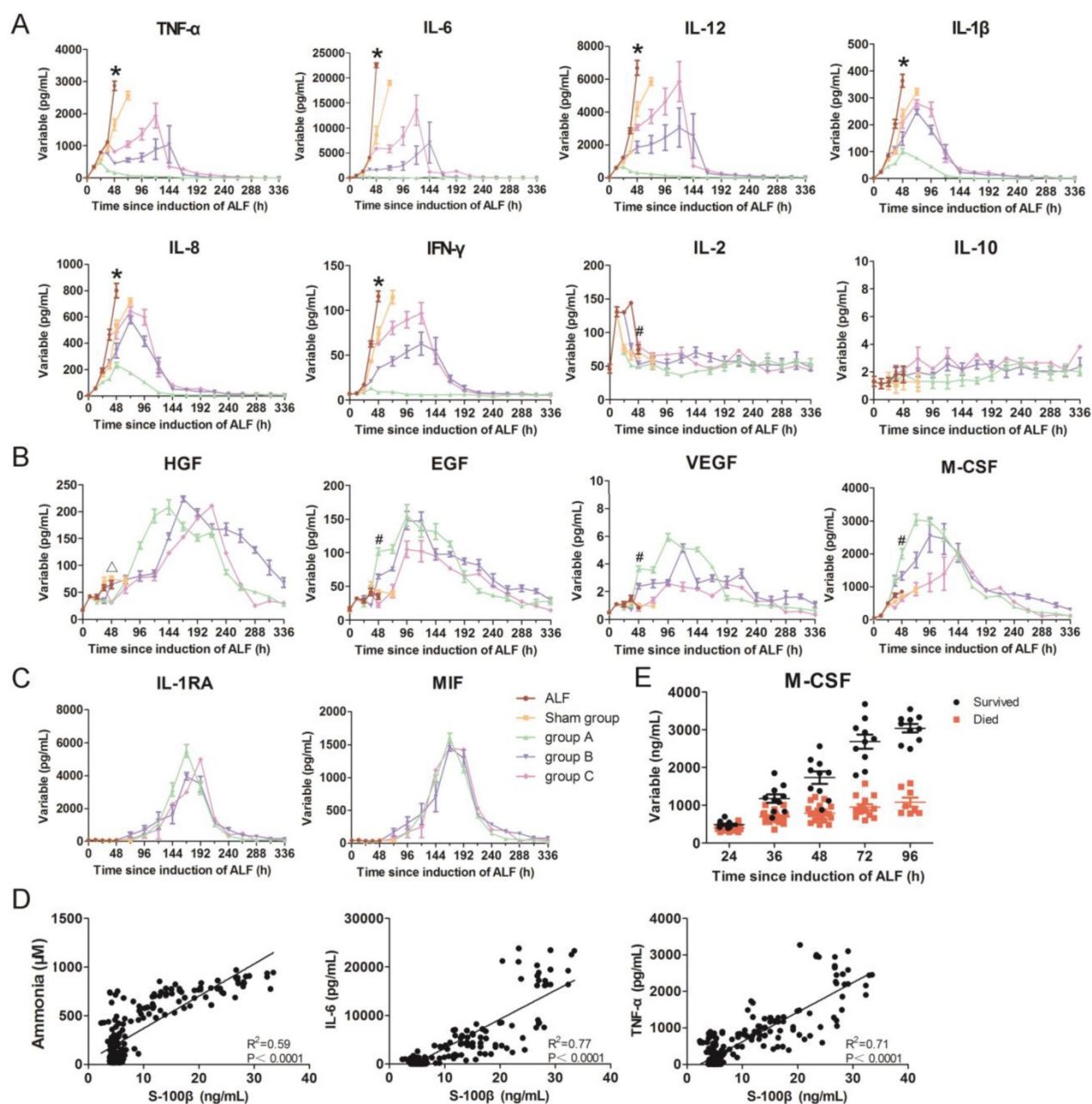


Figure 5. Dynamic changes in inflammatory parameters in monkey blood. (A) Pro-inflammatory cytokines including TNF- α , IL-6, IL-12, IL-1 β , IL-8, IFN- γ , IL-12, and anti-inflammatory cytokine IL-10. **(B)** Growth factors including HGF, EGF, VEGF and colony-stimulating factor M-CSF. **(C)** Other cytokines including IL-1RA and MIF in all groups. **(D)** Correlation curves of serum ammonia, IL-6 and TNF- α level versus S-100 β level. **(E)** Serum M-CSF levels in ALF monkeys (survived, n = 10; died, n = 20). *p < 0.05 sham group, groups A, B, C versus ALF control group;

Discussion

Human hepatocytes are the preferred source of cells for a BAL, but they are currently an impractical source due to limitations in both quantity and availability. Immortalized human hepatoblastoma cell lines like C3A or HepG2 can produce proteins; however, they demonstrate poor metabolism and ammonia clearance [17, 18]. Immortalized C3A cells have been tested in the extracorporeal liver assist device (ELAD); however, no randomized control

trials have shown survival benefit to date and meta-analysis results are inconclusive [19]. Human-induced hepatocytes (hiHep) have potentials for metabolic detoxification, but they need further testing to minimize safety concerns and to reduce costs to meet clinical use [20]. Shi et al. have used hiHep derived from human fetal fibroblasts in a BAL support system in a D-gal-induced model [21]. The hiHep-based BAL treatment could attenuate liver damage, resolve inflammation and enhance liver regeneration; however, it is cumbersome and time-consuming to prepare adequate and high-quality

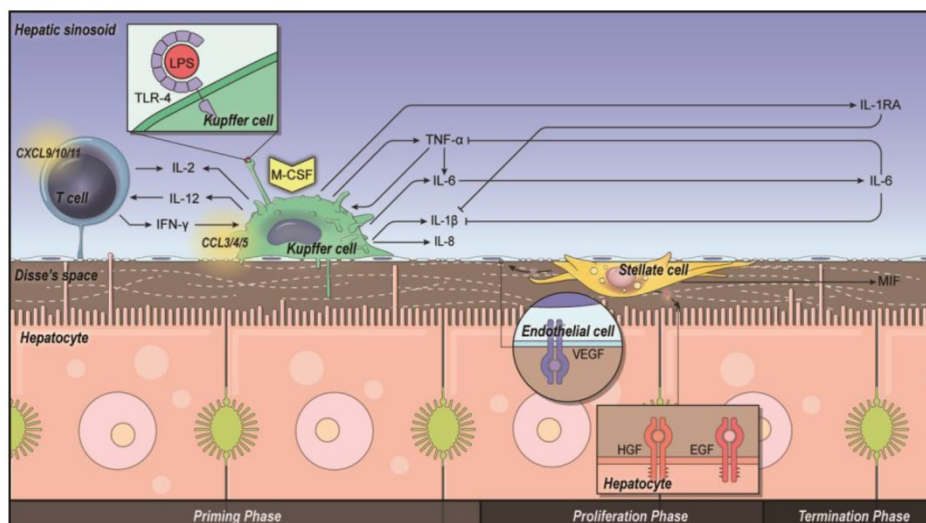


Figure 6. Intercellular interactions and priming, proliferation and termination in liver regeneration. Kupfer cells (KCs) prime T cells, hepatocytes and stellate cells via pro-inflammatory cytokines such as TNF- α and IL-6 (priming phase). Growth factors such as HGF and EGF are released from hepatic stellate cells (HSCs) and extracellular matrix, leading to proliferation of hepatocytes (proliferation phase). Other cytokines such as IL-1RA are released from KCs, and MIF is released from stellate cells, terminating the proliferation process after liver regeneration (termination phase).

cells for emergent patient demands. Freshly isolated primary porcine hepatocytes have more complete metabolic profiles compared to cells lines, especially ureagenesis, glycogenesis and drug metabolism via the cytochrome P450 system. In addition, cell-cell and cell-extracellular matrix interactions are known to be crucial in maintaining specific functions of hepatic cells [22]. A spheroid culture rocker system, the unique system we exploited to form hepatocyte-HUVEC organoids; can improve the viability and metabolic functions of hepatocytes [12]. Before treatment, after putting the hepatocyte organoids into the reservoir, oxygen consumption, albumin production and urea synthesis were evaluated to meet the minimum criteria. The organoid functionality was stable for at least 36 h and still kept high viability and active function after the treatments (Figure S2-S4).

Our data suggest that the survival time of ALF monkeys was increased significantly by SRBAL treatment initiated at 12 h compared to the two control groups (no device treatment or no cell treatment). The benefits of SRBAL therapy included preventive effects and therapeutic effects, and these benefits declined with a delay in the initiation of therapy. And, the sham group without cells prolonged the survival time of animals due to dialysis of the blood by 25 g/L albumin solution across a permeable membrane to remove albumin-bound toxins. SRBAL possessed notable potentials for metabolic detoxification by reducing serum levels of ammonia, bilirubin and cytokines. However, the benefit of SRBAL treatment was more than a

reduction in the toxic effect of drug infusion, otherwise the MST of the sham group should be prolonged obviously because of the early initial treatment time. SRBAL for the treatment of liver disease is relevant from three perspectives: firstly, by reducing the toxic effects of toxins and metabolites; secondly, by inhibiting inflammatory reactions; and thirdly, by providing a microenvironment that is suitable for improving regeneration.

The primary reason for the improved survival of ALF animals after SRBAL treatment is thought to be the prevention of progressive HE [8]. Ammonia is widely

considered as the major pathogenic contributor to cerebral edema and dysfunction [23]. However, the correlation between HE and ammonia concentration is not always consistent [24]. In this study, we pooled all the observations obtained at different time-points and in all experimental groups and found that ammonia concentration correlated with S-100 β level, the neuropathological biomarker (Pearson $R^2 = 0.59$, $P < 0.0001$). In fact, LPS plays a crucial role in the progression of HE in patients with liver disease: it can increase brain water significantly without destroying the anatomical integrity of the BBB [25]. It is quite common that patients with liver disease show tendency to translocation of gut microbiota, which is strongly associated with mortality [26]. In response to LPS, KCs in the liver can be activated through Toll-like receptor-4 (TLR-4) to produce significant amounts of TNF- α . The elevation of TNF- α can self-reinforce to sustain its concentration and activity in the microenvironment and secondarily upregulate secretion of cytokines including IL-6, IFN- γ and IL-1 β , pro-inflammatory cytokines that heavily exacerbate astrocyte swelling and increase ICP [27]. They can also damage endothelial cells and increase vascular permeability, leading to significantly enhanced ammonia concentration, which has toxic effects in the central nervous system. Additionally, cytokines like TNF- α may also reduce levels of branch chain amino acids and increase the peripheral type benzodiazepine receptors in the cortex and striatum [28]. The level of S-100 β was correlated with those of IL-6 (Pearson $R^2 = 0.77$, $P < 0.0001$) and TNF- α (Pearson $R^2 = 0.71$, $P <$

0.0001) as well (Figure 5D). A multiple linear regression model with the dependent variables of ammonia, IL-6 and TNF- α concentration can be established as follows:

$$Y_{S-100\beta} = 0.012X_{\text{ammonia}} + 0.002X_{\text{IL-6}} - 0.006X_{\text{TNF-}\alpha} + 3.972$$

(Pearson $R^2 = 0.83$, $P < 0.0001$),

to predict the S-100 β levels and emergence of HE.

KCs, the specialized macrophages located in the liver, mediate hepatic innate immune defense and promote hepatocyte proliferation after liver injury. Their numbers are regulated during disease progression by the stimulation of M-CSF. According to previous studies, serum M-CSF is an important response to liver injury: M-CSF level increases after partial hepatectomy and acetaminophen-induced ALF. Low serum level of M-CSF is associated with increased patient mortality [29]. In our study, serum M-CSF was increased significantly compared with baseline of healthy monkeys. Lower serum M-CSF was associated with progression of ALF and subsequent death, whereas an increase in serum M-CSF level appeared in those livers that regenerated (Figure 5E). However, the numbers of KCs in the liver were much less in the survival cases; this may be because the increased M-CSF had some effects on activating macrophages in the circulation to proliferate but inhibited migration of mature cells of the immune system into tissue. Serum M-CSF can also be used as a novel prognostic biomarker for α -amanitin/LPS-induced ALF. Administration of M-CSF may have some potential as a therapeutic intervention.

The primary immunological barrier to the use of porcine hepatocytes for SRBAL is hyperacute rejection mediated by naturally occurring cytotoxic antibodies present in the serum of rhesus monkeys [30]. The release of porcine antigens could reach the animals' circulation, stimulating the production of xenoreactive antibodies. Nyberg et al. reported that repetitive exposure of dogs to porcine antigens after BAL treatment resulted in strongly hepatotoxic IgG (150 kD) and IgM (900 kD) xenoantibodies. However, the severe response may be reduced with 65 kD membrane molecular weight cutoff, compared to 200 nm, 10 nm or 400 kD [31-33]. We observed a 3- to 4-fold increase in IgM antibodies in the monkey blood 24 h after drug administration, but there was no further increase after treatment with SRBAL containing porcine hepatocytes. In fact, IgM level declined to normal, while IgG did not show an obvious increase the whole time. The IgM and IgG levels remained unchanged thereafter in the animals without immunosuppression. The reason may be that IgM was the first antibody to appear in response to initial exposure to the LPS, rather than from the

xenogeneic hepatocytes. However, The IgM response was not strong enough to cause maturation of the antibody response and mediate a secondary immune response. Thus, IgG was not generated after antigenic stimulation.

As a xenogeneic cell, primary porcine hepatocytes have other safety concerns, including a means of xeno-zoonosis. For example, PERV, first discovered in 1971 in PK15 cells [34], has been shown to infect the human HEK293 cell line *in vitro* [35]. However, the replication status and clinical consequences of cross-species PERV infectivity is still under debate. The biological safety of treatments based on porcine hepatocytes, such as SRBAL, must be investigated before clinical trials on patients. Nyberg et al. demonstrated that exposure to PERV during extracorporeal therapy is highly correlated with the pore size and composition of the semipermeable membrane used in the device [36]. Therefore, we used well-established and sensitive detection methods, PCR, ddPCR and RT-PCR, to measure PERV DNA and mRNA in blood samples of monkeys treated with SRBAL. Our data suggests that no PERV virus crossed through the 65 kDa semipermeable membrane of the SRBAL device. In addition, negative PERV detection in tissues after 6 h treatment suggested a very low infection risk of PERV in the short duration of SRBAL treatment. Further research about whether PERV infection can be accumulated and be correlated to the treatment interval should be planned.

In conclusion, our study suggests that SRBAL exhibits a remarkable capacity to support liver function by detoxification and suppression of inflammation, leading to liver regeneration and spontaneous recovery of rhesus monkeys with ALF. During the SRBAL treatment, no evidence regarding xenoantigens or PERV infection were observed, suggesting that SRBAL treatment is safe within the conditions of this one-time treatment. Whether a higher cell dose and longer or repeated SRBAL treatments can be safe and improve the survival benefit when starting the treatment later, such as in group B and C, remains to be investigated. Moreover, further research on next-generation models is needed to pave the way for clinical application of SRBAL in the future.

Abbreviations

AD: albumin dialysate; AL: artificial liver; ALB: albumin; ALF: acute liver failure; ALT: alanine aminotransferase; AST: aspartate aminotransferase; BAL: bioartificial liver; BBB: blood-brain barrier; BUN: blood urea nitrogen; EGF: epidermal growth factor; FBS: fetal bovine serum; HE: hepatic

encephalopathy; H & E: hematoxylin and eosin; HGB: hemoglobin; HGF: hepatocyte growth factor; HR: heart rate; HSCs: hepatic stellate cells; HUVECs: human umbilical vein endothelial cells; ICP: intracranial pressure; IFN: interferon; IL: interleukin; IL-1RA: IL-1 receptor antagonist; KCs: Kupffer cells; LPS: lipopolysaccharide; MAP: mean artery pressure; MARS: molecular adsorbents recirculating system; M-CSF: macrophage colony-stimulating factor; MIF: macrophage migration inhibitory factor; MST: median survival time; PBMCs: peripheral blood mononuclear cells; PERV: porcine endogenous retrovirus; PLT: platelet; PT: prothrombin time; RBC: red blood cell; RR: respiratory rate; SRBAL: spheroid reservoir bioartificial liver; TB: total bilirubin; TLR-4: toll-like receptor-4; TNF: tumor necrosis factor; VEGF: vascular endothelial growth factor.

Supplementary Material

Supplementary figures and tables.

<http://www.thno.org/v08p5562s1.pdf>

Acknowledgments

The authors are grateful to Xiujuan Wu, Jing Tang, Zhenggui Du, Xiaoyun Zhang and Guangneng Liao for their valuable assistance in conducting experiments.

Financial support statement

The research leading to these results received funding from National Key Clinical Project, National Natural Scientific Foundations of China (81770618, 81200315), China Postdoctoral Science Foundation Grant (2013T60855), Sichuan Province Science and Technology Support Project (2013SZ0080), and Universities Specialized Research Foundation (20120181110090).

Authors' contributions

YL assisted in conducting experiments, collecting data and writing the manuscript.

QW assisted in conducting experiments, collecting data and analyzing blood samples.

YJW assisted in conducting experiments and collecting data.

CXW assisted in making illustrations.

YTH assisted in conducting experiments.

MYG assisted in conducting experiments.

GY managed animals and performed animal experiments.

LL examined liver pathology.

FC examined liver pathology.

YJS assisted in conducting experiments.

BPA designed the machine and assisted in writing the manuscript.

SLN designed the study and assisted in writing the manuscript.

JB designed the study, supervised experiments and assisted in writing the manuscript.

HB designed the study design and supervised experiments.

Competing Interests

The authors have declared that no competing interest exists.

References

- Bernal W, Wendon J. Acute liver failure. *N Engl J Med.* 2010; 369: 2525-34.
- Davies NA, Banares R. A new horizon for liver support in acute liver failure. *J Hepatol.* 2015; 63: 303-5.
- Kjaergard LL, Liu J, Als-Nielsen B, Gluud C. Artificial and bioartificial support systems for acute and acute-on-chronic liver failure: a systematic review. *JAMA.* 2003; 289: 217.
- Banares R, Nevens F, Larsen FS, Jalan R, Albillos A, Dollinger M, et al. Extracorporeal albumin dialysis with the molecular adsorbent recirculating system in acute-on-chronic liver failure: the RELIEF trial. *Hepatology.* 2013; 57: 1153-62.
- Saliba F, Camus C, Durand F, Mathurin P, Letierce A, Delafosse B, et al. Albumin dialysis with a noncell artificial liver support device in patients with acute liver failure: a randomized, controlled trial. *Ann Intern Med.* 2013; 159: 522-31.
- Brophy CM, Luebke-Wheeler JL, Amiot BP, Khan H, Rimmel RP, Rinaldo P, et al. Rat hepatocyte spheroids formed by rocked technique maintain differentiated hepatocyte gene expression and function. *Hepatology.* 2009; 49: 578-86.
- Nyberg SL, Hardin J, Amiot B, Argikar UA, Rimmel RP, Rinaldo P. Rapid, large-scale formation of porcine hepatocyte spheroids in a novel spheroid reservoir bioartificial liver. *Liver Transpl.* 2005; 11: 901-10.
- Glorioso JM, Mao SA, Rodysill B, Mounajjed T, Kremers WK, Elgilani F, et al. Pivotal preclinical trial of the spheroid reservoir bioartificial liver. *J Hepatol.* 2015; 63: 388-98.
- Chen HS, Joo DJ, Shaheen M, Li Y, Wang Y, Yang J, et al. Randomized Trial of Spheroid Reservoir Bioartificial Liver in Porcine Model of Post-Hepatectomy Liver Failure. *Hepatology.* 2018.
- Zhou P, Xia J, Guo G, Huang ZX, Lu Q, Li L, et al. A Macaca mulatta model of fulminant hepatic failure. *World J Gastroenterol.* 2012; 18: 435-44.
- Li Y, Wang Y, Wu Q, Li L, Shi Y, Bu H, et al. Comparison of methods for isolating primary hepatocytes from mini pigs. *Xenotransplantation.* 2016; 23: 414-20.
- Bao J, Fisher JE, Lillegard JB, Wang W, Amiot B, Yu Y, et al. Serum-free medium and mesenchymal stromal cells enhance functionality and stabilize integrity of rat hepatocyte spheroids. *Cell Transplant.* 2013; 22: 299-308.
- Kanai H, Marushima H, Kimura N, Iwaki T, Saito M, Maehashi H, et al. Extracorporeal bioartificial liver using the radial-flow bioreactor in treatment of fatal experimental hepatic encephalopathy. *Artif Organs.* 2007; 31: 148-51.
- Strauss GL, Christiansen M, Moller K, Clemmesen JO, Larsen FS, Knudsen GM. S-100b and neuron-specific enolase in patients with fulminant hepatic failure. *Liver Transpl.* 2001; 7: 964-70.
- Horai R, Asano M, Sudo K, Kanuka H, Suzuki M, Nishihara M, et al. Production of mice deficient in genes for interleukin (IL)-1 α , IL-1 β , IL-1 α/β , and IL-1 receptor antagonist shows that IL-1 β is crucial in turpentine-induced fever development and glucocorticoid secretion. *J Exp Med.* 1998; 187: 1463-75.
- Calandra T, Roger T. Macrophage migration inhibitory factor: a regulator of innate immunity. *Nat Rev Immunol.* 2003; 3: 791-800.
- Nyberg SL, Rimmel RP, Mann HJ, Peshwa MV, Hu WS, Cerra FB. Primary hepatocytes outperform Hep G2 cells as the source of biotransformation functions in a bioartificial liver. *Ann Surg.* 1994; 220: 59.
- Mavri-Damelin D, Damelin LH, Eaton S, Rees M, Selden C, Hodgson HJ. Cells for bioartificial liver devices: the human hepatoma-derived cell line C3A produces urea but does not detoxify ammonia. *Biotechnol Bioeng.* 2008; 99: 644-51.
- Zheng Z, Li X, Li Z, Ma X. Artificial and bioartificial liver support systems for acute and acute-on-chronic hepatic failure: A meta-analysis and meta-regression. *Exp Ther Med.* 2013; 6: 929-36.
- Huang P, Zhang L, Gao Y, He Z, Yao D, Wu Z, et al. Direct reprogramming of human fibroblasts to functional and expandable hepatocytes. *Cell Stem Cell.* 2014; 14: 370-84.
- Shi XL, Gao Y, Yan Y, Ma H, Sun L, Huang P, et al. Improved survival of porcine acute liver failure by a bioartificial liver device implanted with induced human functional hepatocytes. *Cell Res.* 2016; 26: 206-16.
- Brophy CM, Luebke-Wheeler JL, Amiot BP, Khan H, Rimmel RP, Rinaldo P, et al. Rat hepatocyte spheroids formed by rocked technique maintain

- differentiated hepatocyte gene expression and function. *Hepatology*. 2009; 49: 578-86.
23. Balata S, Olde Damink SW, Ferguson K, Marshall I, Hayes PC, Deutz NE, et al. Induced hyperammonemia alters neuropsychology, brain MR spectroscopy and magnetization transfer in cirrhosis. *Hepatology*. 2003; 37: 931-9.
 24. Qureshi MO, Khokhar N, Shafqat F. Ammonia levels and the severity of hepatic encephalopathy. *Am J Med*. 2003; 114: 188-93.
 25. Shawcross DL, Shabbir SS, Taylor NJ, Hughes RD. Ammonia and the neutrophil in the pathogenesis of hepatic encephalopathy in cirrhosis. *Hepatology*. 2010; 51: 1062-9.
 26. Llorente C, Schnabl B. The gut microbiota and liver disease. *Cell Mol Gastroenterol Hepatol*. 2015; 1: 275-84.
 27. Schmidt-Arras D, Rose-John S. IL-6 pathway in the liver: From physiopathology to therapy. *J Hepatol*. 2016; 64: 1403-15.
 28. Aldridge DR, Tranah EJ, Shawcross DL. Pathogenesis of hepatic encephalopathy: role of ammonia and systemic inflammation. *J Clin Exp Hepatol*. 2015; 5: S7-S20.
 29. Stutchfield BM, Antoine DJ, Mackinnon AC, Gow DJ, Bain CC, Hawley CA, et al. CSF1 Restores Innate Immunity After Liver Injury in Mice and Serum Levels Indicate Outcomes of Patients With Acute Liver Failure. *Gastroenterology*. 2015; 149(e14): 1896-909.
 30. Zhang Y, Shi XL, Han B, Gu JY, Chu XH, Xiao JQ, et al. Immunosafety evaluation of a multilayer flat-plate bioartificial liver. *Am J Med Sci*. 2012; 343: 429-34.
 31. Matsushita T, Amiot B, Hardin J, Platt JL, Nyberg SL. Membrane pore size impacts performance of a xenogeneic bioartificial liver. *Transplantation*. 2003; 76: 1299-305.
 32. Nyberg SL, Amiot B, Hardin J, Baskinbey E, Platt JL. Cytotoxic immune response to a xenogeneic bioartificial liver. *Cell Transplant*. 2004; 13: 783-91.
 33. Nyberg SL, Yagi T, Matsushita T, Hardin J, Grande JP, Gibson LE, et al. Membrane barrier of a porcine hepatocyte bioartificial liver. *Liver Transpl*. 2003; 9: 298-305.
 34. Armstrong JA, Porterfield JS, De Madrid AT. C-type virus particles in pig kidney cell lines. *J Gen Virol*. 1971; 10: 195-8.
 35. Patience C, Takeuchi Y, Weiss RA. Infection of human cells by an endogenous retrovirus of pigs. *Nat Med*. 1997; 3: 282-6.
 36. Nyberg SL, Hibbs JR, Hardin JA, Germer JJ, Persing DH. Transfer of porcine endogenous retrovirus across hollow fiber membranes: significance to a bioartificial liver. *Transplantation*. 1999; 67: 1251.